Exp Brain Res (2003) 149:276–288
DOI 10.1007/s00221-002-1357-5

RESEARCH ARTICLE

Ya-Weng Tseng · John P. Scholz · Gregor Schöner · Lawrence Hotchkiss

Effect of accuracy constraint on joint coordination during pointing movements

Received: 14 February 2002 / Accepted: 15 November 2002 / Published online: 31 January 2003

Abstract Given the number of muscles and joints of the arm, more ways are available to produce an identical hand movement when pointing to a target than are strictly necessary. How the nervous system manages these abundant degrees of freedom was the focus of this study of pointing to targets of low and high indices of difficulty (ID). Two essential features of movement synergies were examined. The first reflects the preferred relations among the outputs of each movement element and was studied through principal component analysis. The second feature of synergy reflects the flexibility of those relationships evidenced by the use of multiple, goal-equivalent solutions to joint coordination. This second feature, which is the main focus of this report, was studied using the uncontrolled manifold approach. Motor abundance was defined operationally as the component of variance of joint combinations that left unchanged the value of important performance variables (goal-equivalent variability, GEV). This variance component was contrasted with the component of variance leading to a change in the value of these variables (non-goal-equivalent variability, NGEV). The difference between GEV and NGEV was evaluated with respect to the performance variables movement extent, movement direction, and path of the arm's center of mass. More than 90% of the variance of joint motions across the pointing trial were accounted for by one principal component, indicating a consistent temporal coupling among most joint motions in a single functional synergy. The flexible nature of this synergy was revealed by the variability analysis. All subjects had significantly higher GEV than NGEV for most of the movement path. Thus, variable patterns of joint coordination did not represent noise but the use of equivalent coordinative solutions related to stabilizing important performance variables. Higher GEV than NGEV was present regardless of the task's ID. One exception was at the time of peak velocity, leading to poorer control of movement extent than movement direction. Increasing the task's ID led to an overall reduction of joint configuraion variance, particularly GEV. These results support earlier work indicating that the use of goal-equivalent solutions to joint coordination is a common feature of the control of this and many other motor tasks. Functionally important performance variables appear to be controlled through flexible but task-specific coordination among the motor elements

Keywords Reaching · Pointing · Motor control · Coordination

Y.-W. Tseng · J. P. Scholz (✉)
Physical Therapy Department and Biomechanics and Movement Science Program, 307 McKinly Laboratory,
University of Delaware, Newark, DE, 19716, USA
e-mail: jpscholz@udel.edu
Tel.: +1-302-8316281
Fax: +1-302-8314234

G. Schöner
Lehrstuhl Theoretische Biologie,
Institut für Neuroinformatik,
Ruhr-Universität Bochum, 44780, Bochum, Germany

L. Hotchkiss
Information Technologies, 032 Smith Hall,
University of Delaware, Newark, DE, 19716 USA

Introduction

This report addresses the nature of movement synergies underlying a pointing task. Movement synergy is a characteristic of most, if not all, functional motor acts (Bernstein 1967; Turvey 1990). Movement synergies are thought to reduce the number of degrees of freedom (DOFs) for which the nervous system must generate explicit plans. The feature of synergies most often emphasized experimentally is that of the preferred relations among the participating movement components. Such relations have been described for a variety of motor tasks (Desmurget et al. 1995; MacPherson 1988; Pelz et al. 2001; Santello and Soechting 2000; Santello et al. 2002; Scholz 1993; Soechting and Lacquaniti 1989; Wang and Stelmach 1998). Principal component analysis (PCA) is one method commonly used to identify such

relationships or patterns of coordination over a time realization of an action or over a range of task parameters (Soechting and Lacquaniti 1989; Scholz 1993; Santello and Soechting 2000; Santello et al. 2002).

A second, less well-studied feature of movement synergy reflects compensatory aspects and/or flexibility of motor coordination. Because of motor redundancy, many solutions to coordinating the joints and muscles are possible to achieve, for example a given hand position during reaching. This abundance of solutions provides a basis for flexible patterns of coordination. The extent to which the nervous system takes advantage of the available motor abundance is unclear, however, and is probably dependent on task constraints. There is, of course, no a priori reason why more than one solution needs to be used across task repetitions. In fact, using a single successful solution might simplify movement planning. However, because the inherent noise of biological systems, as well as small external perturbations, can lead to variations in the outputs of some movement components from their average (expected) outputs on a particular repetition, *selective* changes in the output of other movement components should occur to preserve the overall functional output of the synergy, i.e., the desired hand position. It has been suggested that this second feature of synergy is the most salient feature for biological coordination (Latash et al. 2002). Understanding this feature of synergy requires the study of variations of patterns of motor coordination. It is this feature that is the primary emphasis of the present report.

Some researechers have emphasized the need to effectively reduce the excess DOFs available to solve a motor task, viewing motor redundancy as a control "problem." It has been suggested that the purported redundancy problem is solved by applying various cost functions to constrain the choice of joint and muscle combinations (Cruse et al. 1990, 1993; Rosenbaum et al. 1996, 1999). For example, Desmurget and colleagues have argued that such constraints lead to a fixed or constant terminal arm configuration across repetitions when reaching to targets (Desmurget and Prablnac 1997; Desmurget et al. 1998; Grea et al. 2000). In contrast, a growing body of literature suggests that the nervous system takes advantage of the abundant solutions for coordinating muscles and joints available to it (Scholz and Schöner 1999; Scholz et al. 2000, 2001, 2002; Latash et al. 2001; Domkin et al. 2002; Reisman et al. 2002; Tseng et al. 2002). A consistent finding from these studies has been that a range of goal-equivalent solutions to coordinating motor elements were used, specifically those which were consistent with stable values of important performance variables. In contrast, combinations of motor elements that would change the values of these variables were restricted. The extent to which this strategy was used depended on the nature of environmental and task constraints under which the performance occurred. Therefore, it appears that the nervous system applies a robust approach to manage the superfluous DOFs rather than selectively "freezing" them. This finding of flexible motor patterns to achieve stable values of important task variables is consistent with the second feature of synergy already described here.

To further address these issues, we asked the following questions in a study of pointing to targets:

1. Can the coordination of joint motions across time during pointing be accounted for by a single movement synergy?
2. Is flexible coupling of joint motions across task repetitions a characteristic feature of the pointing synergy and, if so, is that coupling affected by the accuracy requirement of the task?
3. Is the flexibility of joint coupling differentially associated with the control of different performance variables?
4. Do the arms differ in how joint motions are coordinated during pointing, revealed either by the average relationship among joint motions across time during pointing or by the flexibility of joint coupling across repetitions?

To address the first feature of synergy described here, we performed a PCA on the joint angles across time within a trial. The uncontrolled manifold (UCM) hypothesis, proposed initially by Schöner (1995), was applied in the present study to understand the second feature of synergy, i.e., the extent to which flexible patterns of joint combinations were used to control specific performance variables important to task success. The UCM hypothesis links the control of a multielement system to the structure of variability of its individual components, allowing the understanding of how multiple DOFs are organized to achieve a desired goal. The hypothesis enables the test of a control law linking the coordination of motor components to the stability of important performance variables such as the hand's movement path. This proposed control law selectively restricts variations of the joint configuration that lead to changes away from the desired values of important performance variables. At the same time, multiple, goal-equivalent solutions to joint coordination are allowed, consistent with the second feature of synergies described here. Two recent studies of reaching tasks that evaluate this hypothesis report evidence for this style of control, i.e., the selective use of goal-equivalent joint combinations that produce a stable hand path throughout the movement (Domkin et al. 2002; Tseng et al. 2002). In one study, the extent of using goal-equivalent solutions depended on the interaction between the availability of vision and the arm's dominance (Tseng et al. 2002).

Task constraints were varied by using targets having different indices of task difficulty (IDs). It is well known that performance of a rapid reaching movement is directly related to the accuracy demand of the task. The movement distance and the width of the target are most commonly studied to address this issue. Movement time can be expressed as a logarithmic function of target size and movement distance, which is often referred to as

"Fitts law" (Fitts 1954). Movement time has been found to be longer, with a proportionally lengthened deceleration time, when the object to be reached becomes smaller (Berthier et al. 1996; Smyrnis et al. 2000). In addition, the variability of the hand and wrist joint path was reported to be reduced when pointing to a smaller object (Soechting 1984). However, this finding was found to be present only when the hand approached the target, not during the initial launching phase of the movement (Soechting 1984; Kudoh et al. 1997).

Data from Soechting's study (1984) has shown that the relationship between the shoulder and elbow joint became more consistent when reaching toward the smaller target, suggesting that a more fixed solution to joint coordination may be used when reaching with higher-accuracy constraints. In that study, however, a pair-wise comparison of joint angles provided limited insight about interjoint coordination, because redundancy was not an issue. The present study sheds further light on this issue in the context of three-dimensional (3D) pointing movements involving coordination of ten joint angles.

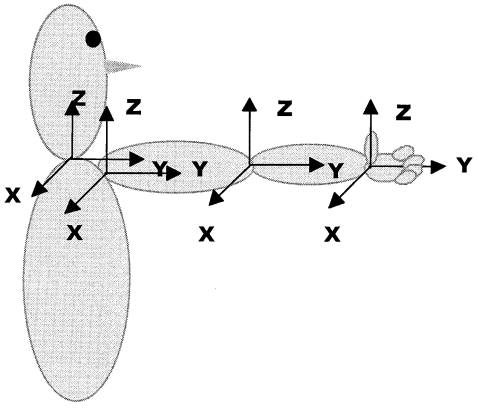

Fig. 1 The right arm's posture during the calibration procedure for joint-angle calculations. The local coordinate systems are centered at the sternoclavicular-, glenohumeral-, elbow-, and wrist-joint centers. These are coordinate systems for reconstructing joint angles. The *x*-dimension points to the right of the subject, the *y*-dimension points forward, and the *z*-dimension points upward in the calibration posture. The same arrangements apply for the left arm

Methods and materials

Subjects

Nine healthy subjects (three men and six women, 26.56 ± 5.3 years old) volunteered for the study. All the subjects were naive about the purpose of the study. They had no neurological or musculoskeletal deficits and had normal or corrected-to-normal vision. All volunteers were right-hand dominant according to initial self-report, although one subject appeared to be ambidextrous according to the Edinburgh handedness inventory (Oldfield 1971), which was administered to all subjects to confirm their handedness. Because the data of this subject was not different from that of other subjects, we still included his results in the analyses. Subjects signed consent forms approved by the Human Subjects Review Board, University of Delaware.

Setup

Six infrared cameras were placed in a semi-circle anterior and lateral to the subject to record arm movements at 120 Hz (VICON; Oxford Metrics). The cameras were calibrated prior to each data collection. Subjects sat on an adjustable-height, high-backed chair. Chair height was adjusted so that each subject's arm was perpendicular to a tabletop that was placed in front of them, with the elbow at 90° of flexion and the forearm resting on the tabletop in the starting arm location. This arm position was marked on the table for replication across trials. The edge of the table was placed snugly against the subject's abdomen. The table was used to support the hand and distal forearm in the starting position and to locate the targets. The snug position of the table against the subject's abdomen served to prevent lower trunk motion, and subjects were reminded to move only the arm and scapula when pointing to the targets. Although the task did not require trunk movement, these precautions were taken to ensure that the trunk did not participate, because our geometric model did not account for trunk motions. None of the subjects used their trunk.

Individual reflective markers were attached with adhesive to the skin overlying the following bony landmarks: (1) sternal notch (center of rotation for modeled scapula motion); (2) just inferior to the lateral edge of acromion process; (3) lateral and medial epicondyles of the humerus (elbow axis); (4) just distal to ulnar and radial epicondyles (wrist axis). Four reflective markers were mounted on each of four rigid bodies that were made of Orthoplast. These were used to track motions of the scapula, arm, forearm, and hand segments. One was mounted on the top of the subject's shoulder, medial to the acromion process. The arm array was attached to the lateral aspect of the upper arm and the forearm array was attached to the lower half of the forearm. A custom-made hand splint that subjects wore allowed tracking of the hand's motion. The splint had two reflective markers mounted on its dorsum. Two additional markers were attached to a 4-inch piece of wooden bar that served as a pointer and that was rigidly attached to the hand splint. The pointer's placement was adjusted so that the distal marker on the pointer tip was aligned with the subject's index finger when fully extended. However, the finger was kept in a flexed position against the palm when pointing, so that pointing was done with the pointer.

The target was a 5-cm-diameter rubber ring (large target) or a 1.3-cm-diameter bead (small target), attached to an adjustable horizontal extension of a vertical metal rod that was screwed into a flat base. The target was placed at a 45° angle contralateral to a line directed forward from the acromion process of the shoulder of the arm used to point. Target distances were standardized as 95% of the distance between the acromion process of the shoulder and the proximal interphalangeal joint of the index finger, measured with the arm fully extended. This ensured that the arm was not fully extended with the pointer tip positioned at the center of the target. Target height was set to 7-cm above the height of the shoulder in sitting.

Subject calibration

A static calibration posture of the arm was recorded prior to each data collection. This arm calibration was the basis for joint-angle calculations in a body-centered coordinate frame (see the section Joint-angle calculations for more details). All joint angles were defined as zero degrees at this calibration posture (see Fig. 1). The subjects were told to hold their arm perpendicular to the trunk with their thumb facing upwards, the wrist kept in neutral, the elbow fully extended, and shoulder at 90° of flexion. The position was adjusted to meet these criteria by the experimenter.

Instructions

Prior to each experiment, subjects were asked to assume the same starting position, which was checked by the experimenter. The starting position had the hand placed on the table at a distance of 90% of their forearm length, anterior to the subject's shoulder. Their elbow rested comfortably on the table at an angle of 90°. They were instructed to perform each trial as follows: "After hearing the experimenter's 'go' signal, move the pointer tip in one continuous motion to the center of the designated target at a fast, but comfortable speed while being as accurate as possible. Try to keep the speed consistent across all trials." Subjects were given as many trials of practice as necessary to determine an appropriate speed. In no case was this more than five trials.

Experimental conditions

Two conditions of different index of difficulty (ID) were studied. The ID was calculated using Fitts' law (Fitts 1954):

$$\mathrm{ID} = \log_2(\mathrm{D}/\mathrm{W})$$

where D is the distance to the target center and W is the width of the target. In the low-ID condition, the target was a 5-cm-diameter rubber ring attached to a metal post with an ID=3.6. In the high-ID condition, the circular target was replaced to a 1.3-cm-diameter bead with an ID=5.6. For both conditions, subjects looked at the target throughout the experiment. Twenty trials of reaching in each of the low- and high-ID conditions were performed in a random order for each arm. The order in which arm was tested was also pseudorandomly chosen by the experimenter.

Data analysis

Reconstruction of marker positions

Reflective marker identification and reconstruction of the 3D marker positions from the six camera views were done using VICON software. Further processing of the kinematic data was performed using customized MATLAB programs. The marker positions were filtered at 5 Hz using a forward and reverse low-pass, 2nd-order Butterworth filter. The start of the movement was determined as the time of the first crossing of the acceleration profile at 5% of the peak acceleration. An automatic algorithm was used to choose the earliest onset and latest movement termination among three dimensions: medial-lateral (x), anterior-posterior (y), and vertical (z).

Joint-angle calculations

Joint angles were obtained based on local coordinate systems defined at each joint in the subject calibration position (Fig. 1). Details of the method, which used the Söderkvist and Wedin (1993) algorithms for obtaining the necessary rotation matrices, are described in detail elsewhere (Scholz et al. 2000). The new extension used in this study was to account for scapula motion (Tseng et al. 2002). This motion was modeled as motions of the rigid body positioned on top of the shoulder with respect to the fixed trunk and occurring about an axis located at the sternoclavicular joint. The model was determined to be adequate by having the subjects perform controlled scapular motions. The amount of reconstructed motions of these defined scapular angles was found to be consistent with the scapular motions that the subjects were asked to perform.

The joint angles measured during the pointing task were: (1) scapular elevation-depression; (2) scapular upward-downward rotation; (3) scapular abduction-adduction; (4) glenohumeral joint flexion-extension; (5) glenohumeral joint internal-external rotation; (6) horizontal abduction-adduction of the glenohumeral joint; (7) elbow flexion-extension; (8) forearm pronation-supination; (9) wrist radial-ulnar deviation; and (10) wrist flexion-extension. The elbow axis used for calculating elbow flexion-extension was rotated from that in the subject calibration position (Fig. 1) so that the x-axis was oriented along a line passing between the medial and lateral epicondyles of the humerus. The joint-angle trajectories were then normalized to 100% based on the previously defined trial onset and termination times, using a cubic spline algorithm in MATLAB.

Selection of trials

We selected trials for the analysis that showed the most consistent timing of the movement path and the least end-point error. Specifically, we calculated the mean movement time across trials based on the previously defined onset and termination of the movement. Trials were included if their movement time was within the ±1.75 standard deviations (SD) of the mean movement time. The mean end-point position of the pointer tip across trials was also calculated. Trials having end-point positions within ±1.75 SD of the mean end-point were included. A comparison algorithm was written in MATLAB in order to find trials that meet both criteria. This resulted in the use, on average, of 15 trials per condition.

Principal component analysis

We evaluated the preferred relationships between the joint motions involved in this reaching and pointing task by performing a PCA. PCA attempts to identify a smaller set of uncorrelated linear combinations of the original variables such that the set of new variables, or principal components (PCs), captures most of the information of the original variables (Dunteman 1989). In the present experiments, ten joint angles that contribute to movement of the hand in space were studied to determine whether all joint angles were linked in a single functional synergy or if there was evidence for multiple synergic combinations of the joint motions. For example, one can imagine that there might be separate synergies related to, for example hand transport and to final adjustment of hand position at the target. One limitation of PCA, however, is that the meaning of each PC is not always directly apparent and requires user interpretation, which may not be trivial. Consider, for example, a case where two PCs each explain a substantial amount of the joint-angle variance. This result would suggest that two independent synergies are acting to coordinate joint motions in performing the task. However, which aspect of the movement does each of these PCs relate to? This may or may not be readily apparent, leading to problems in interpretation.

We performed a PCA separately for each trial of each subject's data and then examined the reliability of the results across trials. First, the covariance matrix of the time-normalized (0–100%) trajectories of ten joint angles was obtained. Then, the eigenvectors (weighted contributions of each angle to each PC) and eigenvalues (variance of each PC) were obtained. All analyses were performed using MATLAB. The matrix of eigenvectors was then rescaled to obtain factor loadings ($\mathbf{U}=\mathbf{V}\Lambda^{1/2}$, where $\mathbf{U}$ is the matrix of rescaled eigenvectors, $\mathbf{V}$ is the original matrix of eigenvectors scaled to unit length, and Λ is a diagonal matrix, with diagonal elements set to the eigenvalues ordered to correspond to their paired eigenvectors; Dunteman 1989). These loadings provide an indication of the extent to which each of the original joint angles covaries with each of the resulting PCs. We based our analysis on the covariance matrix of joint angles rather than the correlation matrix to make it more consistent with our UCM analysis. Thus, the relative size of the weights or loadings of a particular joint angle on a given PC should be interpreted with caution: joint angles with more excursions (e.g., elbow) will naturally contribute more to the variance than angles with less motion (e.g., wrist). Instead, we determined on which PC a given joint angle had its highest factor weight.

The proportion of variance explained by each eigenvector or PC was obtained as the eigenvalue for that PC divided by the sum of

the eigenvalues for all ten PCs. We based the choice of how many (new) independent variables were adequate to explain the joint-angle variations across the reaching movement on the criterion that the included PCs should account for 95% of the total variance. In addition, we determined the percentage variance of each individual joint angle that was explained by this minimum set of PCs. This was obtained as the sum of squared weighting factors of each row (angle) for those PCs that explained most of the variance, divided by the sum of squared weighting factors of that row for all PCs (Dunteman 1989).

Uncontrolled manifold

The UCM approach provides a method to decompose the variance of joint-angle combinations across task repetitions, performed under identical conditions, into two orthogonal components. Unlike PCA, this decomposition is performed with respect to specific hypotheses about the control of variables that appear to be important for the task's performance. One component of the variance of joint combinations is that which leads to a change in the value of a performance variable under consideration, e.g., hand position, and is referred to as non-goal-equivalent variability or NGEV. The second component is the variance of joint combinations that is consistent with stable values of the performance variable (goal-equivalent variability, GEV). Goal-equivalent variance reflects the extent to which motor abundance is used by the nervous system to control or achieve stable values of a performance variable (Schöner 1995). The relative magnitudes of GEV and NGEV, which we refer to as the structure of joint configuration variance, can differ for different performance variables. This is because the geometric model relating joint angle space to performance variable space for different performance variables is different, e.g., pointer tip position versus position of the arm's center of mass (CM). As such, this method provides insights about the nervous system's relative control of different performance variables as well as the extent to which motor abundance is used to achieve that control. In this study, the structure of joint configuration variance was evaluated with respect to the control of the extent and direction of pointer tip movement, as well as the path of the arm's CM.

Consider the possibility that the central nervous system (CNS) uses a control law that attempts to produce an ideal or optimal sequence of joint configurations to achieve a stable hand movement to a target, i.e., by invoking additional constraints in the form of cost functions (Cruse et al. 1990; Rosenbaum et al. 1996). In this case, goal-equivalent solutions to joint coordination are not expected, and all joint configuration variability is expected to be NGEV. That is, to the extent that the control system is not perfect, noise in the neuromuscular system will lead to some variation in the joint configuration across repetitions that leads to some alteration of the hand path. If the CNS is particularly poor at controlling the variable under consideration, NGEV will be relatively high.

If, instead, the CNS takes advantage of the motor abundance available to it, using a range of goal-equivalent joint combinations, then joint configuration variability is expected to be present as GEV. Because biological control systems are somewhat noisy, some of the joint configuration variance will also show up as NGEV. However, one would expect NGEV to be relatively low and GEV to be more than NGEV if control of the performance variable under consideration is important and if exploitation of motor abundance is an important aspect of that control. To the extent that the CNS attempts to invoke this control strategy for a given performance variable but is not very good at it, then both GEV and NGEV may be high and relatively equal. Thus, comparisons of the relative magnitude of components of joint configuration variability can provide insights about the nature of CNS control of functional motor tasks.

The first step in applying the UCM approach is to develop a geometric model that links the space of performance variables with the space of joint angles. For a hypothesis about controlling the spatial position of the hand, the k = 3D hand position is expressed as a combination of n=10 joint angles, the joint configuration. Having the geometric model, a linear estimate of all goal-equivalent joint-angle combinations, i.e., those that are consistent with a given 3D-hand position, can be obtained. This estimate is obtained by calculating the null space of the Jacobian matrix (a matrix relating changes in the joint-angle configuration to changes in a performance variable, based on the geometric model; see Scholz et al. 2000 for details). In this example, goal-equivalent combinations can be represented as an $n–k$ or seven-dimensional (e.g., 10–3) subspace embedded in the ten-dimensional coordinate space of the joint angles. We refer to such subspaces as uncontrolled manifolds, because any combination of joint angles lying within the UCM is consistent with the desired hand position. Thus, there is no need for the CNS to specify a particular value. In practice, other factors or task constraints may lead to some restriction of that space.

At each percentage of the time-normalized hand path, the mean (across trials) joint configuration was used to calculate the Jacobian. The null space of the Jacobian was then obtained using MATLAB. This computation returns the basis vectors corresponding to dimensions of the UCM in joint angle space. To analyze the extent to which joint configuration variance lies within a given UCM at any point in time, the vector of ten joint angles for each task repetition at the appropriate point in time was projected onto each dimension of the UCM and those dimensions orthogonal to the UCM. The variance (across repetitions) of the projection onto the UCM provides an estimate of GEV, while the variance of the projection orthogonal to the UCM provides an estimate of NGEV. Each variance component is then normalized by the number of DOFs for presentation and statistical anaysis. For example, for the hypothesis about control of the 3D path of the CM, GEV is divided by 7 (ten angles, 3-DOF CM spatial position) while NGEV is divided by 3 to yield the variance per DOF. For the hypothesis about control of movement extent, which is a one-dimensional hypothesis represented by a vector pointing from the starting position to the target center, the UCM is nine-dimensional and GEV is divided by 9. Finally, for the hypothesis about control of movement direction, which is composed of two DOFs or directions orthogonal to the vector pointing from the starting position to the target center, GEV is divided by 8, while NGEV is divided by 2 to yield the variance per DOF. Details of the mathematical method as applied to the analysis of similar tasks have recently been reported (Scholz et al. 2000; Tseng et al. 2002).

Dependent variables

Principal components. The combined PCs that explained more than 95% of the variance of the joint angles for a given trial were identified. The factor loadings, derived by rescaling the eigenvectors, were evaluated for their reliability across trials by calculating fixed-effects model intraclass correlation coefficients (Shrout and Fleiss 1979). Finally, the percentage of variance of each joint angle accounted for by the dominant PCs was calculated.

Components of joint configuration variance. The two components of joint configuration variance, GEV and NGEV, calculated at every 1% of the movement period, were of primary interest for evaluating the flexibility of the movement synergy used to perform the pointing task. These variance components were calculated at every 1% of the movement with respect to the following performance variables: (1) the extent and direction of pointer-tip movement; (2) the 3D position of the arm's CM. To better facilitate statistical analyses, GEV and NGEV were then averaged over the periods of 0–20% (early phase), 30–50% (middle phase), and 70–90% (late phase) of the movement path, as well as at movement termination (100%), and evaluated with respect to each of the control hypotheses (i.e., movement extent or direction, or CM position).

Kinematic variables. The following kinematic variables were also examined:

1. Movement time: duration from the onset to the end of the movement
2. Peak movement velocity: movement velocity was calculated by taking the first derivative of the pointer tip's path using central differences method. Then, a customized program written in MATLAB was applied to find the maximal velocity and the time of this maximum
3. Time to peak velocity: the time to peak velocity was expressed as a percentage (%) of the total movement time
4. Path variability of movement extent and direction: After the 3D path of pointer-tip coordinates represented in the global coordinate system were normalized to 100%, these coordinates were transformed into a new coordinate system. The origin of this new coordinate system was at the starting location of the pointer tip and the new *x*-axis was defined by the line passing through the starting position and the center of the target of each condition. The direction of the *z*-axis of this transformed system was obtained by taking the cross product between a temporary unit vector pointing parallel to the global *x*-axis (defined in Fig. 1) in the positive direction from the starting position to a unit vector pointing along the new *x*-axis. The cross product of a unit vector pointing along the new *z*-axis with a unit vector pointing along the new *x*-axis yielded the direction of the new *y*-axis. Movement extent was defined as movement along the transformed *x*-axis, from starting position to the target center, consistent with the definition of Gordon et al. (1994). Movement direction was represented by directional deviations from that path, i.e., movement along the new *y*- and *z*-dimensions. Variability along the new *x*-axis was defined as the variability of movement extent, whereas the mean variability along the new *y*- and *z*-axes was defined as directional variability. This variability was then averaged across 0–20%, 30–50%, 70–90% of the movement, along with the value at 100%, yielding measures of variability of the performance variable at the same movement phases as the measures of joint configuration variability (GEV and NGEV)
5. Path variability of CM: this was calculated by taking the standard deviation of the arm's CM position at each percentage of the normalized movement time, and averaged across the same periods as those described in 4. Reconstruction of the arm's CM position was done using the anthropometric data from Winter (1979) to find the location of the center of mass as a percentage of the longitudinal length for each segment (i.e., scapula, upper arm, forearm, and hand). Then, the weighted sum (the mass of each segment relative to the mass of the arm) of these segmental CM locations determined the CM position of the whole arm

Independent variables

The independent variables directly manipulated in the experiment were the arm with which subjects pointed (right and left) and the index of difficulty (low and high).

Statistical analysis

The hypotheses were analyzed with repeated-measure analyses of variance (ANOVA) using the SPSS statistical package. Separate analyses were performed to analyze the effects of independent variables on measures related to the extent and direction of the pointer tip and of the arm's CM. Factors in the ANOVA included the independent variables and the components of variance (GEV and NGEV). Each ANOVA was performed separately on data for four different phases of the movement (early, middle, late, and terminal pointer position).

Results

The results for movement kinematics will be presented first, followed by the analysis of features of movement synergy of pointing using (1) PCA and (2) the UCM analysis of joint configuration variability to test different control hypotheses, i.e., related to different performance variables. Last, we present the variability of the actual performance variables to show their relative consistency with the UCM analysis results.

Pointer-tip kinematics

Contrary to expectations, the index of task difficulty did not affect the mean movement time ($P>0.3$; see Table 1), the magnitude of peak velocity ($P>0.4$), nor the time to reach peak velocity ($P>0.4$; Table 1). There were also no arm effects on any of these variables.

Relative temporal coupling among joint angles during pointing

Table 2 presents for each arm and ID combination the mean percentage (± SD) of joint-angle variance across time (within trial) accounted for by the first and second principal components, averaged across trials and then subjects. The results of the PCAs indicate that the joint motions tended to be linked as one movement synergy. Close to 95% of the variance of the joint angles for all conditions was explained by the first principal component (PC1), while the second principal component accounted for approximately 4% of the variance. Also presented in the table are the mean intraclass correlation coefficients (ICCs; ± SD) across subjects. This statistic assessed the reliability of the eigenvectors of the PCA across all trials for a subject, which was then averaged across subjects. The reliability of the eigenvectors of both PC1 and PC2 was high for each ID and arm combination, being more than 0.99 in all cases. This indicates that the weighting of

Table 1 Mean±SD of movement time, peak velocity, time to peak velocity (TPV), expressed as a percentage of movement time, and distance moved for each experimental condition

Movement variables	Low		High	
	Right arm	Left arm	Right arm	Left arm
Movement time (s)	1.026±0.07	0.990±0.05	1.032±0.07	1.011±0.06
Peak velocity (m/s)	1.41±0.127	1.37±0.102	1.36±0.118	1.33±0.097
TPV (% of MT)	35.3±1.54	35.7±1.59	36.3±1.60	34.8±1.35

Table 2 Mean± SD of percent of variance explained and intraclass correlation coefficient (ICC), depicting the reliability of joint angle weights across trials for the first (PC1) and second (PC2) largest principal components, averaged across subjects. ICC value is for reliability of k observations using a fixed-effects model (Shrout and Fleiss 1979)

Arm	Left arm				Right arm			
ID	Low ID		High ID		Low ID		High ID	
PC	PC1	PC2	PC1	PC2	PC1	PC2	PC1	PC2
%Variance explained	94.93±0.80	4.59±0.75	95.82±0.55	3.78±0.51	94.74±0.83	4.86±0.81	95.23±0.97	4.32±0.90
ICC	0.999±0.0003	0.997±0.0016	0.999±0.0004	0.996±0.0031	0.999±0.0004	0.996±0.0023	0.999±0.0003	0.992±0.0152

joint angles on the PCs was relatively consistent from trial to trial.

Although PC1 accounted for most of the variance of joint angles during the movement, not all joint angles loaded heavily on this principal component. When examining individual joint contributions, it became clear that the proximal joints were most strongly linked on this synergy while the more distal joints contributed less strongly, particularly when reaching with the right arm across the body in the high-ID condition. The scapular, shoulder, and elbow angles were found to load most heavily on PC1 on no less than 94%, and in most cases on 100% of all trials, with minimal differences across the arm by ID combinations. In contrast, the forearm pronation, wrist extension, and wrist abduction angles loaded most heavily on PC1 much less frequently. The two wrist angles were most strongly associated with PC1 on only 62% of the trials, on average, across subjects. For forearm pronation, this was the case on less than 20% of the trials. Also, for forearm pronation, there was more variability across arms (5.6% and 27.8% of the time this angle had its highest loading on PC1 when pointing with the left and right arm, respectively).

This proximal to distal difference is also somewhat apparent for the relative amount of each joint angle's variability that was accounted for by PC1, which is presented in Table 3. With two exceptions, more than 90% of the variance of the proximal joint angles was accounted for by PC1. The amount of a joint angle's variance accounted for by PC1 decreased for the more distal joints, and this percentage was relatively variable across subjects for the wrist joint motions. The forearm's rotation (forearm pronation, PRO, in Table 3) was, however, only moderately accounted for by PC1 and there was much variability across subjects. An ANOVA revealed no effects of ID or interactions of joint angles with ID. However, there was a significant main effect of joint angle in the percentage of variance accounted for by PC1 ($F_{9, 72}$=19.34, P<0.0001).

Flexible patterns of joint coordination underlying control of different performance variables

Joint coordination underlying control of movement direction

The previous analysis addressed the average relationship among the joint-angle changes across time within a trial. The UCM analysis allowed determination of the extent to which the joint angles were coupled in a flexible manner and the relationship of that coupling to the control of different performance variables. Unlike the previous analysis, this analysis was performed across trials, separately at each point in normalized time. Fig. 2 presents the components of joint configuration variability related to control of the hand's movement direction. The averaged results across arms are presented because there was no arm difference. As introduced earlier, GEV in this

Table 3 Percentage of the variation of each joint angle explained by PC1 alone. (*SC1* scapular abduction, *SC2* scapular elevation, *SC3* scapular outward rotation, *SH1* shoulder horizontal adduction, *SH2* shoulder flexion, *SH3* shoulder internal rotation, *ELB* elbow extension, *PRO* forearm pronation, *WR1* wrist extension, *WR2* wrist radial deviation)

Condition ID	*N*	Joint angles								
		SC1	SC2	SC3	SH1	SH2	SH3	ELB	PRO	WR1	WR2
L→R: low ID	1300	89.22±2.92	94.07±4.41	96.69±1.62	99.01±0.72	91.95±7.91	92.86±8.45	82.50±8.06	45.88±26.8	88.78±11.2	87.66±11.6
L→R: high ID	1340	91.03±2.44	94.01±3.44	95.46±3.05	99.02±0.51	91.02±6.51	94.91±5.24	85.16±6.5	48.60±31.5	78.44±24.5	81.75±22.4
R→L: low ID	1340	91.15±3.95	91.44±7.47	95.30±4.04	98.54±1.26	92.55±8.62	92.82±5.07	87.01±6.5	53.52±33.2	82.99±14.8	76.23±24.7
R→L: high ID	1330	92.14±2.81	93.01±4.59	88.71±21.7	98.99±0.88	87.30±19.8	95.18±3.94	88.99±4.40	47.85±34.7	78.34±18.4	74.62±21.3

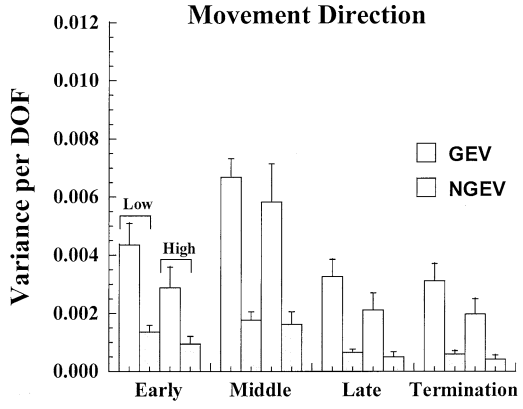

Fig. 2 The mean components of joint configuration variance (radians squared) underlying control of movement direction in the low- and high-indices of difficulty (ID) conditions, averaged across arms. The conditions are indicated by adjacent *pairs of bars* at each phase of the movement path. Each *bar* represents the mean value of variance across trials and subjects. The *error bars* are standard errors of the means across subjects (*n*=9). *Open bars*, goal-equivalent variability, *GEV*; *shaded bars*, non-goal-equivalent variability, *NGEV*

figure represents goal-equivalent joint configurations that are consistent with a stable movement direction, whereas NGEV represents the variability of the joint configuration leading to a change in movement direction. As the figure indicates, GEV was more than NGEV for the control of movement direction throughout the course of movement (early: $F_{1,8}$=26.56, P=0.001; middle: $F_{1,8}$=79.52, P<0.0001; late: $F_{1,8}$=20.76, P<0.01; termination: $F_{1,8}$= 20.04 P<0.01).

Joint coordination underlying control of movement extent

The relationship between GEV and NGEV for controlling movement extent was qualitatively similar to that of the movement direction in the early ($F_{1,8}$=24.16, P=0.001), late ($F_{1,8}$=20.72, P<0.01) and termination ($F_{1,8}$=23.34, P=0.001) phases of the movement (Fig. 3). However, the range of non-goal-equivalent joint combinations increased substantially at the middle phase of the movement such that NGEV was more than GEV ($F_{1,8}$=8.96, P<0.05; cf. Fig. 2 and Fig. 3). Moreover, movement direction was always associated with more GEV than movement extent at the late phase ($F_{1,8}$=19.66, P<0.01) and at movement termination ($F_{1,8}$=16.01 P<0.01). These particular results also were consistent across the different IDs.

Effect of index of task difficulty

Although GEV was higher than NGEV in both the high-ID and low-ID conditions, this difference was significantly smaller during the last half of pointing in the high-ID compared with the low-ID condition with respect to

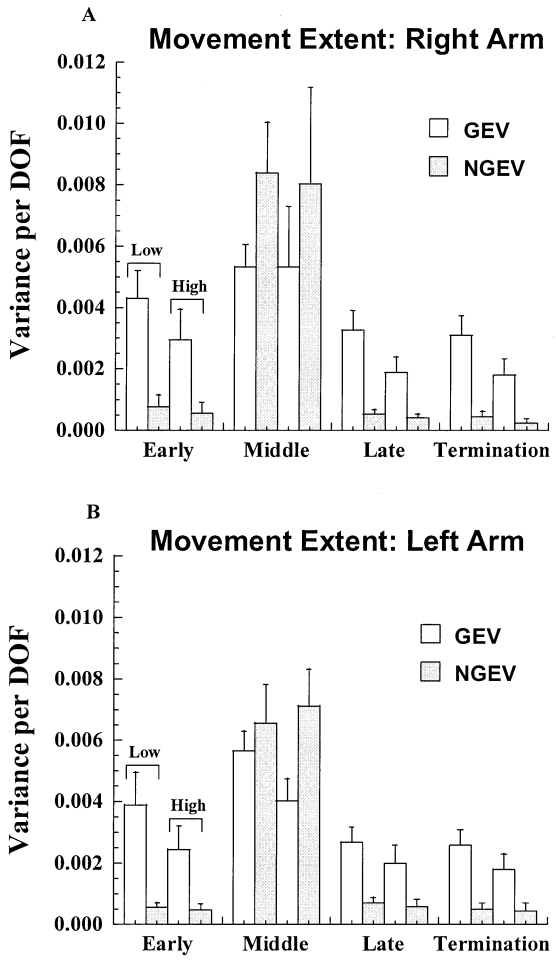

Fig. 3A, B The mean components of joint configuration variance (radians squared) underlying control of movement extent in the low- and high-ID conditions for **A** the dominant arm and **B** the nondominant arm. Each *bar* represents the mean value of variance across trials and subjects. The *error bars* are standard errors of the means, averaged across subjects (*n*=9). *Open bars*, GEV; *light gray bars*, NGEV

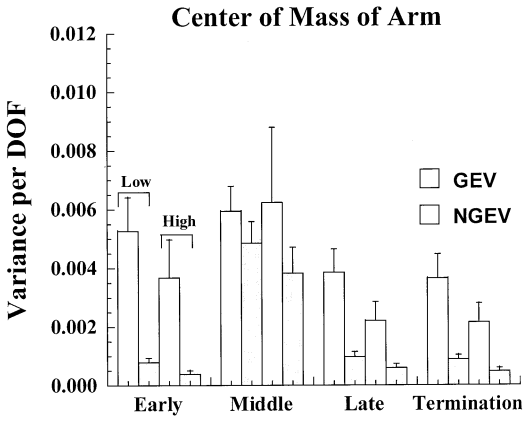

Fig. 4 The mean components of joint configuration variance (radians squared) underlying control of the arm's center of mass path in the low- and high-ID conditions for the dominant arm. Each *bar* represents the mean value of variance across trials and subjects. The *error bars* are SEMs, averaged across subjects (*n*=9). *Open bars*, GEV; *light gray bars*, NGEV

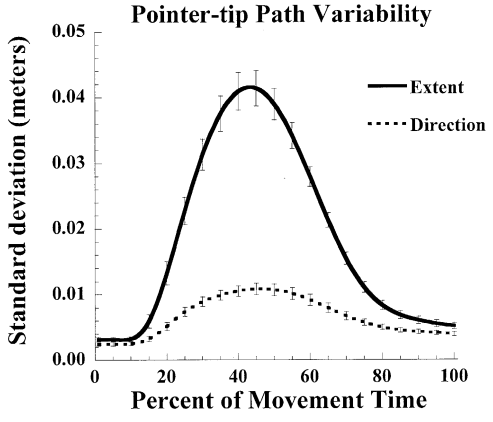

Fig. 5 The SD (meters) of movement path. *Solid lines*, movement extent; *dashed lines*, movement direction. Results from the low-ID conditions are presented, collapsed across arms. The *error bars* are calculated at every 5% of the normalized movement

control of both movement direction (late: $F_{1,8}$=22.22, P<0.01; termination: $F_{1,8}$=19.86, P<0.01) and movement extent (late: $F_{1,8}$=16.65, P<0.01; termination: $F_{1,8}$=17.49, P<0.01). The effect of ID on the difference between GEV and NGEV was not significant in the early (P>0.08) and middle (P>0.2) phases of the movement.

For the control of movement extent, both GEV ($F_{1,8}$=17.45, P<0.005) and NGEV ($F_{1,8}$=8.04, P<0.05) were reduced when pointing with the dominant, right arm in the high-ID compared with the low-ID condition. For the left arm, only GEV decreased when pointing in the high-ID compared with low-ID condition, and only toward the end of the movement (GEV, $F_{1,8}$=9.55, P<0.05; NGEV, P>0.5; see the termination phase in Fig. 3A, B). No such arm differences were present for similar comparisons related to the control of movement direction.

Joint coordination underlying control of arm CM position.

The nature of joint configuration variability underlying the control of the arm's CM position was very similar to that for control of movement extent of the pointer tip. Goal-equivalent variability was significantly higher than NGEV at the early ($F_{1,8}$=17.08, P<0.01) and late phases ($F_{1,8}$=15.56, P<0.01) and at the terminal movement phase ($F_{1,8}$=15.11, P<0.01). In contrast, GEV and NGEV did not differ significantly in the middle phase of the movement.

Both GEV and NGEV underlying control of the CM position were reduced in the high-ID compared with the low-ID condition, but only for the right arm (Fig. 4; late: GEV: $F_{1,8}$=11.73, P<0.01; NGEV: $F_{1,8}$=12.15, P<0.01; termination: GEV: $F_{1,8}$=13.75, P<0.01; NGEV: $F_{1,8}$= 18.19, P<0.01).

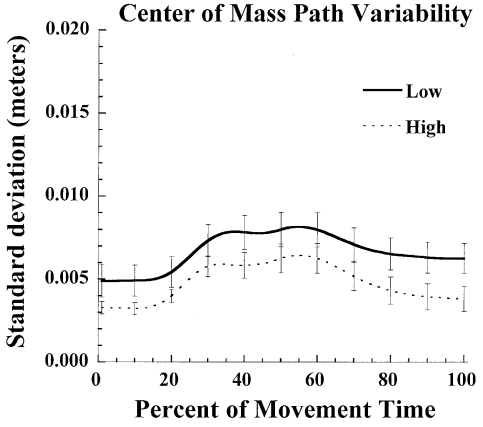

Fig. 6 The SD (meters) of the arm's CM path for each condition, collapsed across arms. *Solid lines*, low-ID condition; *dashed lines*, high-ID condition. The *error bars* are calculated at every 5% of the normalized movement

Stability of performance variables

Figure 5 illustrates the SD of the extent and direction of the pointer-tip's movement in the low index of difficulty condition averaged across arms. Both movement components were more variable from 20 to 80% of the movement period. This was especially so for movement extent (solid line). Movement direction (dashed line) was consistently more stable than movement extent throughout the entire movement (early: $F_{1,8}$=21.46, P<0.01; middle: $F_{1,8}$=285.51, P<0.001; late: $F_{1,8}$=74.15, P<0.001; termination: $F_{1,8}$=14.10, P<0.01), but particularly at the middle of the movement, near the time of peak velocity. This latter finding was consistent with the differences in the magnitude of GEV and NGEV for the control of movement direction and extent at this phase of the movement (cf. Fig. 2, 3).

Control of both movement extent and direction was found to be more consistent for the right, dominant arm than for the left, nondominant arm when the index of difficulty was increased. The variability of movement extent on the dominant side decreased when pointing to the high-ID target at the late phase (low vs high ID: 0.0148±0.00096 m vs 0.0077±0.00093 m: $F_{1,8}$=32.86, P<0.0001) and at movement termination (low vs high: 0.0056±0.00060 m vs 0.0033±0.0003 m: $F_{1,8}$=29.99, P=0.001). The same effect was found for variability of movement direction for the right arm (late: low vs high: 0.0092±0.00055 m vs 0.0041±0.00038 m: $F_{1,8}$=59.60, P<0.0001; termination: low vs high: 0.0042±0.00043 m vs 0.0027±0.00027 m: $F_{1,8}$=18.79, P<0.01). In contrast, there was no reduction in the variability of either movement extent or movement direction with increased ID in the nondominant arm (P>0.1).

The path of the arm's CM was less variable when task difficulty was increased (high-ID; Fig. 6), except around the middle phase of the movement, where there was more inconsistency among the subjects. Both arms demonstrated a similar reduction of CM path variability in the high-ID condition. However, the dominant arm's CM was less variable than that of the nondominant arm in the late phase of movement ($F_{1,8}$=6.02, P<0.05) and at movement termination ($F_{1,8}$=5.32, P=0.05).

Discussion

The results of the present study generally provide positive answers to the questions posed in the Introduction.

Temporal aspects of the arm synergy for pointing

One principal component, representing a linear combination of the ten joint angles, accounted for approximately 95% of the variance of those angles across time. In addition, at least 85% of the variance of all but one joint angle was explained by PC1. This indicates that there was a consistent temporal coupling of the joint motions from the beginning to the termination of the reach. The finding of a single movement synergy underlying the temporal coupling of the joint motions across the reaching task could be considered somewhat surprising. Separate movement synergies related to hand transport and terminal hand adjustment have been frequently suggested, especially for reaching and grasping tasks (Jeannerod 1981, 1984, 1990; Marteniuk et al. 1990; Gentilucci et al. 1992). The transport component is usually described as being more ballistic and of a feedforward nature, whereas the grasp component utilizes information such as the size and shape of the object to preshape the fingers and involves sensorimotor adjustments to "home in" (Jeannerod 1981, 1984). Different movement synergies have also been observed for shaping the hand or coordinating finger forces during grasping (Santello and Soechting 2000; Santello et al. 2002), and in studies of reaching and pointing movements (Desmurget et al. 1995; Wang 1999).

If we had required subjects to grasp an object rather than simply point to a target, a second synergy might have been more likely in the current study. Moreover, we asked subjects to make one uncorrected movement. On the other hand, Desmurget et al. (1995) have reported a tight coupling between most of the joints of the arm when performing reaching and grasping in three-dimensions, consistent with our finding. The somewhat weaker relationship of the distal joint movements to the synergy captured by PC1 in the present experiment may reflect subtle adjustments of the hand trajectory toward the target. This finding is consistent with earlier reports of Soechting (1984), who found that wrist abduction-adduction motion to be only loosely related to motion of more proximal joints. The relationship of distal joint motion to that of more proximal joints was, however, much stronger in our study.

One limitation of the PCA method is that the results require subjective analysis. As the number of PCs needed to account for the data increases, so does the difficulty in providing clear interpretations of the finding. Fortunately,

this was not an issue in the current study. Nonetheless, our finding that one principal component accounted for most of the temporal change in joint motion can be deceiving. The high reliability of the PC vectors across repetitions indicates that the general nature of the temporal coupling of the joints across the movement trajectory was consistent. It does not imply that the actual values of those angular changes were invariant from moment to moment across repetitions. Indeed, our second method, the UCM approach, revealed that the joint coupling was indeed flexibly related to the control of different performance-related variables.

Use of goal-equivalent joint combinations was evident in controlling a reaching task

Unlike PC analysis, the UCM approach relates the variability of joint combinations across task repetitions to the value of specific performance-related variables. As such, the results of this analysis can be objectively related to specific control hypotheses. In this experiment, we examined the structure of joint configuration variability related to the control of the motion of the hand and the arm's CM. By structure, we mean how overall joint configuration variability across trials is partitioned with respect to values of a performance variable at each point along the movement path; i.e., how much of that variance led to a change in those values (non-goal-equivalent component) and how much was associated with flexible patterns of coordination that preserved those values (GEV). In this study, a range of goal-equivalent joint combinations was a characteristic feature of the control of both the pointer tip and CM movement paths. That is, most joint configuration variability had little effect on these movement paths. This finding is consistent with other recent findings (Scholz et al. 2000, 2001; Domkin et al. 2002; Reisman et al. 2002; Tseng et al. 2002). It suggests that the use of goal-equivalent joint configurations serves a useful purpose because, in principal, only one sequence of joint combinations could work (see Scholz et al. 2000).

The higher-accuracy requirement of the small target, i.e., high ID, led to an overall reduction in the range of joint configurations used to control the hand's movement path only during the latter half of the hand's movement path. The finding is consistent with different ID effects reported by others (Soechting 1984; Berthier et al. 1996; Kudoh et al. 1997; Smyrnis et al. 2000), while extending the work of Soechting (1984) by indicating that a global reduction in the motion variability of all DOFs occurs when reaching toward a smaller target.

We should note that our manipulation of the ID of pointing was not as successful as intended. In contrast to a number of studies showing an effect of the task's ID on movement time (Fitts 1954, 1964; Berthier et al. 1996; Ricker et al. 1999; Smyrnis et al. 2000), lengthening of neither the total movement time nor the deceleration phase was not a consistent feature of reaching to the smaller target. This difference may be associated with several factors. First, we asked our subjects to keep the movement speed consistent across all trials. Although this instruction was intended to apply within, not across conditions, in hindsight the way the instruction was provided may have misled subjects to interpret the instruction to mean the latter. Nevertheless, a recent study of 3D pointing using similar instructions to those of the current study also failed to find an effect of target size on movement time (Kudoh et al. 1997). In addition, our task involved 3D reaching, while most studies invoking Fitts' Law have been one- or two-dimensional tasks. It has been shown that the conventional Fitts' model does not completely explain the speed and accuracy relationship for a 3D movement (Murata and Iwase 2001). Nonetheless, we found that the ID manipulation had its greatest effect during the deceleration phase of pointing, consistent with the results of previous studies on reach-and-grasp movements (Soechting 1984; Berthier et al. 1996; Kudoh et al. 1997). And despite the weak effect on movement time in the current experiment, the ID manipulation did reveal quantitative changes in the structure of joint configuration variability, some of which were arm-dependent. Indeed, the observed decrease in joint configuration variability related to ID was present only after the peak velocity of movement.

Joint coordination and the control of different performance variables

While the structure of joint configuration variability was similar for all three performance variables studied, an exception occurred in the middle phase of pointing, near the time of peak movement velocity. There, the relative amount of GEV compared with NGEV increased for control of movement direction, while GEV and NGEV were not different for control of movement extent or the movement path of the arm's CM. Thus, the UCM approach can reveal distinctions in the control of different performance variables, based on the coordination underlying that control. This fact has also been shown in a number of other tasks (Scholz et al. 2000, 2001). Near the time of peak velocity, where interaction torque is probably the highest (Hollerbach and Flash 1982), the coordination of the arm is apparently focused on minimizing deviations of the hand from the straight-line path toward the target (see Rosetti et al. 1995; Desmurget et al. 1997). At the same time, simultaneous control of the hand's exact location along that path and the position of the CM are apparently more difficult and, perhaps, not as critical to final target acquisition. We would predict that this difference in the control of movement extent and direction should disappear for tasks involving the interception of objects at a particular location in space.

Consistent with these results, variability of the pointer tip's movement along the desired path (i.e., representing the extent of movement) was always higher (SD≈4.5 cm) than variability of the off-axis motion (i.e., movement

direction: SD<1 cm). As far as we know, this is the first evidence of differences in joint coordination underlying previously reported differences in the control of movement extent and movement direction (Gordon et al. 1994; Ghez et al. 1997; Messier and Kalaska 1997). However, whether extent and direction are controlled independently, as some authors have suggested, cannot be determined from the present results. A study of reaching to multiple targets with varying distances and spatial directions will be necessary to further explore this control distinction.

Arm differences in pointing

Differences between the arms for this task were found to be minimal. Differences were revealed in the velocity profiles of the hand and in the structure of joint configuration variability related to the control of movement extent and the arm's CM position. The manipulation of ID had a stronger effect on the right arm than on the left arm, resulting in an overall reduction of both GEV and NGEV. In contrast, no such effect was found for the left arm in relation to control of the arm's CM, and only GEV decreased for control of movement extent.

The dynamic-dominance hypothesis proposed by Sainburg (2002) may help account for our findings on the variability of joint configuration. According to this hypothesis, the manual asymmetry arises when a hand's desired trajectory is transformed into the required arm dynamics. Control of the dominant arm is apparently marked by comparatively better use of interactive torque to assist the arm movements (Sainburg and Kalakanis 2000), as well as when adapting to a novel dynamic environment (Sainburg 2002). On the one hand, the observed arm differences in the current experiment were only apparent toward the end of reaching and not at the time of peak movement velocity where interaction torque is highest. On the other hand, the reduction of NGEV for the right hand could reflect its ability to compensate for interaction torque occurring near the time of peak velocity when pointing to the high-ID target, thus minimizing inconsistency of the hand path. That the left arm did not show a similar reduction in the high-ID condition may reflect less skill at compensating for this torque as previously reported.

Acknowledgements This research was supported by grant IBN-0078127 awarded to Dr. Scholz from the Behavioral Neuroscience Division of the National Science Foundation.

References

Bernstein NA (1967) The coordination and regulation of movements. Pergamon, London

Berthier NA, Clifton RK, Gullapalli V, McCall DD, Robin DJ (1996) Visual information and object size in the control of reaching. J Mot Behav 28: 187–197

Cruse H, Wischmeyer E, Brüwer M, Brockfeld P, Dress A (1990) On the cost functions for the control of the human arm movement. Biol Cybern 62: 519–528

Cruse H, Bruwer M, Dean J (1993) Control of three- and four-joint arm movement: strategies for a manipulator with redundant degrees of freedom. J Mot Behav 25: 131–139

Desmurget M, Prablanc C (1997) Postural control of three-dimensional prehension movements. J Neurophysiol 77: 452–464

Desmurget M, Prablanc C, Rossetti Y, Arzi M, Paulignan Y, Urquizar C, Mignot JC (1995) Postural and synergic control for three-dimensional movements of reaching and grasping. J Neurophysiol 74: 905–910

Desmurget M, Rossetti Y, Jordon M, Meckler C, Prablanc C (1997) Viewing the hand prior to movement improves accuracy of pointing performed toward the unseen contralateral hand. Exp Brain Res 115: 180–186

Desmurget M, Grea H, Prablanc C (1998) Final posture of the upper limb depends on the initial position of the hand during prehension movements. Exp Brain Res 119: 511–516

Domkin D, Laczko J, Jaric S, Johansson H, Latash ML (2002) Structure of joint variability in bimanual pointing tasks. Exp Brain Res 143: 11–23

Dunteman GH (1989) Principal component analysis. Sage, London

Fitts PM (1954) The information capacity of the human motor system in controlling the amplitude of movement. J Exp Psychol 47: 381–391

Fitts PM, Peterson JR (1964) Information capacity of discrete motor-responses. J Exp Psychol 67: 103–112

Gentilucci M, Chieffi S, Scarpa M, Castiello U (1992) Temporal coupling between transport and grasp components during prehension movements: effects of visual perturbation. Behav Brain Res 47: 71–82

Ghez C, Favilla M, Ghilardi MF et al. (1997) Discrete and continuous planning of hand movements and isometric force trajectories. Exp Brain Res 115: 217–233

Gordon J, Ghilardi MF, Ghez C (1994) Accuracy of planar reaching movements. I. Independence of direction and extent variability. Exp Brain Res 99: 97–111

Grea H, Desmurget M, Prablanc C (2000) Postural invariance in three-dimensional reaching and grasping movements. Exp Brain Res 134: 155–162

Hollerbach JM, Flash T (1982) Dynamic interactions between limb segments during planar arm movement. Biol Cybern 44: 67–77

Jeannerod M (1981) Intersegmental coordination during reaching at natural visual objects. In: Long J, Baddeley A (eds) Attention and performance IX. Erlbaum, Hillsdale, NJ, pp 153–168.

Jeannerod M (1984) The timing of natural prehension movements. J Mot Behav 16: 235–254

Jeannerod M (1990) The neural and behavioral organization of goal-directed movements. Clarendon, Oxford

Kudoh N, Hattori M, Numata N, Maruyama K (1997) An analysis of spatiotemporal variability during prehension movements: effect of object size and distance. Exp Brain Res 117: 457–464

Latash ML, Scholz JP, Danion F, Schöner G (2001) Structure of motor variability in marginally redundant multifinger force production tasks. Exp Brain Res 141: 153–165

Latash ML, Danion F, Scholz JP, Zatsiorsky V, Schöner G (2002) Approaches to analysis of handwriting as a task of coordinating a redundant motor system. Hum Mov Sci In press

Macpherson JM (1988) Strategies that simplify the control of quadrupedal stance. II. Electromyographic activity. J Neurophysiol 60: 218–231

Marteniuk RG, Leavitt JL, MacKenzie CL, Athenes S (1990) Functional relationships between grasp and transport components in a prehension task. Hum Mov Sci 9: 149–176

Messier J, Kalaska JF (1997) Differential effect of task conditions on errors of direction and extent of reaching movements. Exp Brain Res 115: 469–478

Murata A, Iwase H (2001) Extending Fitt's law to a three-dimensional pointing task. Hum Mov Sci 20: 791–805

Oldfield RC (1971) The assessment and analysis of handedness: the Edinburgh Inventory. Neuropsychologia 9: 97–113

Pelz J, Hayhoe M, Loeber R (2001) The coordination of eye, head, and hand movements in a natural task. Exp Brain Res 139: 266–277

Reisman DS, Scholz JP, Schöner G (2002) Coordination underlying the control of whole body momentum during sit-to-stand. Gait Posture 15:45–55

Ricker KL, Elliott D, Lyons J et al. (1999) The utilization of visual information in the control of rapid sequential aiming movements. Acta Psychol 103: 103–123

Rosenbaum DA, Meulenbroek RGJ, Vaughan J (1996) Three approaches to the degrees of freedom problem in reaching. In: Wing AM, Haggard P, Flanagan JR (eds) Hand and brain. Academic, San Diego, CA, pp 168–185

Rosenbaum DA, Meulenbroek RGJ, Vaughan J (1999) Remembered positions: stored locations or stored postures? Exp Brain Res 124: 503–512

Rossetti Y, Desmurget M, Prablanc C (1995) Vectorial coding of movement: vision, proprioception, or both? J Neurophysiol 74: 457–463

Sainburg RL (2002) Evidence for a dynamic-dominance hypothesis of handedness. Exp Brain Res 142: 241–258

Sainburg RL, Kalakanis D (2000) Differences in control of limb dynamics during dominant and nondominant arm reaching. J Neurophysiol 83: 2661–2675

Santello M, Soechting JF (2000) Force synergies for multifingered grasping. Exp Brain Res 133: 457–467

Santello M, Flanders M, Soechting JF (2002) Patterns of hand motion during grasping and the influence of sensory guidance. J Neurosci 22: 1426–1435

Scholz JP (1993) The effect of load scaling on the coordination of manual squat lifting. Hum Mov Sci 12: 427–459

Scholz JP, Schöner G (1999) The uncontrolled manifold concept: identifying control variables for a functional task. Exp Brain Res 126: 289–306

Scholz JP, Schöner G, Latash ML (2000) Identifying the control structure of multijoint coordination during pistol shooting. Exp Brain Res 135: 382–404

Scholz JP, Reisman D, Schöner G (2001) The effect of varying task constrains on the control structure of standing from sitting. Exp Brain Res 141: 485–500

Scholz JP, Danion F, Latash ML, Schöer G (2002) Understanding finger coordination through analysis of the structure of force variability. Biol Cybern 86: 29–39

Schöner G (1995) Recent developments and problems in human movement science and their conceptual implications. Ecol Psychol 7: 291–314

Shrout PE, Fleiss JL (1979) Intraclass correlation coefficient: uses in rater reliability. Psych Bull 86: 420–428

Söderkvist I, Wedin PA (1993) Determining the movements of the skeleton using well-configured markers. J Biomech 26: 1473–1477

Soechting JF (1984) Effect of target size on spatial and temporal characteristics of a pointing movement in man. Exp Brain Res 54: 121–132

Soechting JF, Lacquaniti F (1989) An assessment of the existence of muscle synergies during load perturbations and intentional movements of the human arm. Exp Brain Res 74 :535–548

Smyrnis N, Evdokimidis I, Constantinidis TS, Kastrinakis G (2000) Speed–accuracy trade-off in the performance of pointing movements in different directions in two-dimensional space. Exp Brain Res 134: 21–31

Tseng Y, Scholz JP, Schöner G (2002) Goal-equivalent joint coordination in pointing: effect of vision and arm domince. Mot Control 6: 183–207

Turvey MT (1990) Coordination. Am Psychol 45: 938–953

Wang J, Stelmach GE (1998) Coordination among the body segments during reach-to-grasp action involving the trunk. Exp Brain Res 123: 346–350

Wang X (1999) Three-dimensional kinematic analysis of influence of hand orientation and joint limits on the control of arm postures and movements. Biol Cybern 80: 449–463

Winter D (1979) Biomechanics of Human Movement. Wiley & Sons, New York